Anisotropic Azimuthal Power and Temperature Distribution as a Driving Force for Hydrogen Redistribution

M.G.Mankosa, C.J.Piotrowski, M.N.Avramova, A.T. Motta, and K.N.Ivanov
[1]Department of Mechanical and Nuclear Engineering
The Pennsylvania State University
Reber Building, University Park, PA 16802, USA
mgm5145@psu.edu, cjp5169@psu.edu, mna109@engr.psu.edu, atm2@psu.edu, kni1@engr.psu.edu

S.Stafford, R.L.Williamson
Idaho National Laboratory
Idaho Falls, Idaho, USA
shane.stafford@inl.gov, richard.williamson@inl.gov

ABSTRACT

The reactor environment, in which nuclear fuel operates, requires improved multi-dimensional fuel and cladding simulation and analysis to accurately describe fuel behavior. The high-fidelity fuel performance code BISON was developed at Idaho National Laboratory (INL) to address this need. BISON is a three-dimensional finite-element based fuel performance code. In the high temperature environment of a reactor, the zirconium in the cladding undergoes waterside corrosion in primary water, releasing hydrogen in the process. Some of this hydrogen is absorbed by the cladding. Once hydrogen is absorbed in the cladding, its distribution is extremely sensitive to temperature, stress and concentration gradients. Hydrogen migrates down temperature and concentration gradients and at a high enough concentration, precipitates as hydrides which can embrittle the cladding. This paper describes a development effort to validate the hydrogen distribution prediction capabilities of the BISON code. The project is divided into two primary sections: first, using a high fidelity multi-physics coupling to accurately predict temperature gradients as a function of radial, azimuthal, and axial directions (r, θ, and z), and using experimental data to validate a previously developed analytical hydrogen transport and hydride precipitation model implemented in BISON.

Key Words: Multi-Physics, MPACT, CTF, BISON, Hydrogen

1 INTRODUCTION

The reactor environment, in which nuclear fuel operates, requires improved multi-dimensional fuel and cladding simulation and analysis to accurately describe fuel behavior. The high-fidelity fuel performance code BISON was developed at Idaho National Laboratory (INL) to address this need. BISON is a three-dimensional finite-element based fuel performance code that can model temperature distributions, fission product swelling, densification, thermal and irradiation creep, mechanical properties and fission gas production [1].

In the high temperature environment of a reactor, the zirconium alloy fuel cladding undergoes waterside corrosion in primary water, releasing hydrogen in the process. Some of this hydrogen is absorbed by the cladding. Once hydrogen is absorbed in the cladding, its distribution is extremely sensitive to temperature, stress and concentration gradients. Hydrogen migrates down temperature and concentration gradients and at a high enough concentration, precipitates as hydrides, which can embrittle the cladding.

This paper describes a development effort to validate the hydrogen distribution prediction capabilities of the BISON code. The goal of this project is to use a high fidelity multi-physics coupling to accurately

predict temperature gradients as a function of radial, azimuthal, and axial directions (r, θ, and z), and to use experimental data to validate a previously developed analytical hydrogen transport and hydride precipitation model implemented in BISON when subjected to such gradients. The (r, z) capabilities have been demonstrated previously (see references [2] and [3]). This paper focuses on the predictive capabilities of the code for the distribution of hydrogen and hydrides in (r, θ) geometry.

1.1 Multi-Physics Coupling

1.1.1 CTF-DeCART-BISON

Penn State developed a multi-physics coupling, which employed a combination of the multi-group neutron transport code DeCART and the sub-channel code COBRA-TF (CTF) [2]. DeCART (Deterministic Core Analysis based on Ray Tracing) is a whole-core, high-fidelity neutron transport code for PWR and BWR calculations. DeCART uses a two-dimensional (2D) method of characteristics (MOC) approach to solve the neutron flux in the x-y direction and a one-dimensional (1D) diffusion method to solve in the z direction. DeCART used the HELIOS 47 group cross sections library for its nuclear data. [4] CTF (Coolant Boiling in Rod Arrays-Two Fluid) is a Penn State University (PSU) maintained multi-dimensional sub-channel thermal hydraulics code [5][6], which currently is being utilized in the Department of Energy (DOE) Consortium for Advanced Simulation of LWR (CASL) project for high-fidelity core thermal-hydraulic calculations. BISON, DeCART, and CTF were coupled using an independent Python script that ran DeCART and CTF inputs and passed information between the codes. The code coupling then output several parameters of interest over the axial, radial and azimuthal directions. This coupled output was then input into a two-dimensional (r, θ) BISON model. An area of interest was selected, and the CTF-DeCARTdata was taken from that area and used as boundary conditions for the BISON model. The system coupling diagram can be viewed in Figure 1.

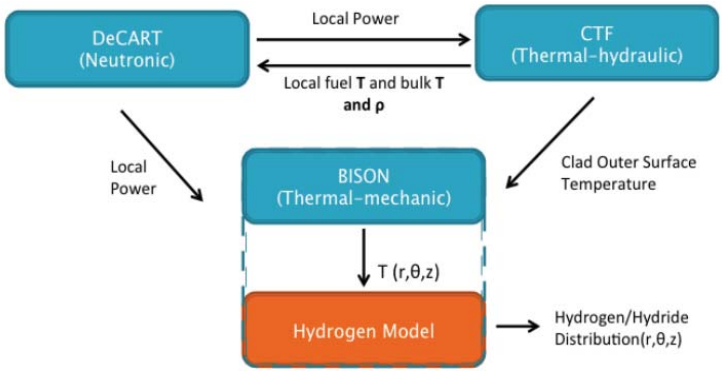

Figure 1: CTF-DeCART-BISON coupling diagram [2]

1.1.2 CTF-MPACT

Moving forward with this project, an alternate multi-physics package will be employed for creation of the boundary conditions for the BISON input. This is the MPACT-CTF coupling developed by the University of Michigan and Oak Ridge National Lab (ORNL) within the CASL program. This coupling uses Michigan Parallel Characteristics based Transport (MPACT), which is a University of Michigan neutronics code, and CTF. MPACT uses the 2D/1D method to find a neutron flux solution in a similar manner to DeCART; however, MPACT also has a three-dimensional (3D) MOC transport solver available. For this combination, an internal coupling scheme was employed, using Lightweight Integral Multi-physics Engine (LIME) and the Data Transfer Kit (DTK) to process and transmit the information between MPACT and CTF. [7] A visualization of the coupling can be seen in Figure 2.

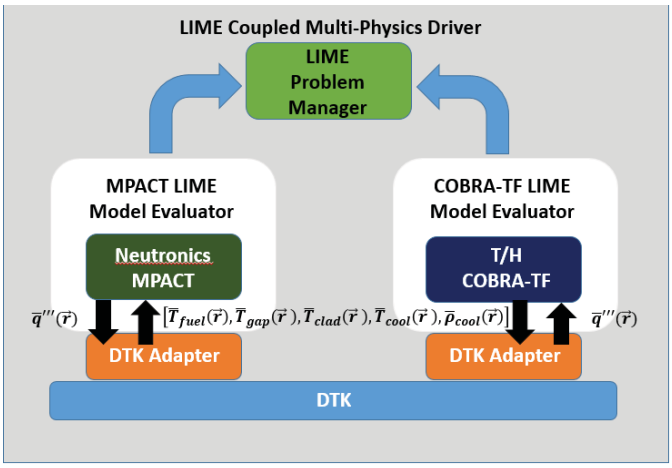

Figure 2: CTF-MPACT coupling diagram [7]

1.2 CTF-DeCART-BISON Hydrogen Distribution Testing

1.2.1 Model Description of CTF-DeCART Coupled Calculations

Several cases were created to test the capability of the previously developed hydrogen redistribution model to reproduce observed instances of hydrogen concentration in response to azimuthal temperature gradients. Two main cases are considered in which azimuthal temperature variations are established by an asymmetric distribution of fuel rod enrichment around the fuel rod of interest. The results obtained demonstrate that using multi-dimensional temperature and power distributions from DeCART/CTF, the hydrogen transport and precipitation model in BISON is able to predict inhomogeneous hydrogen distribution and hydride formation in fuel cladding. Appropriate experimental data is to be used for quantitative validation of the established multi-physics high-fidelity modeling and simulation methodology once detailed enough data becomes available.

To test the hydrogen modeling capabilities of the BISON code, models were created that employed geometries, and pin positioning that would induce large azimuthal temperature gradients. Sub-assemblies of 16 pins in a 4x4 pattern were used as shown in Figure 3.

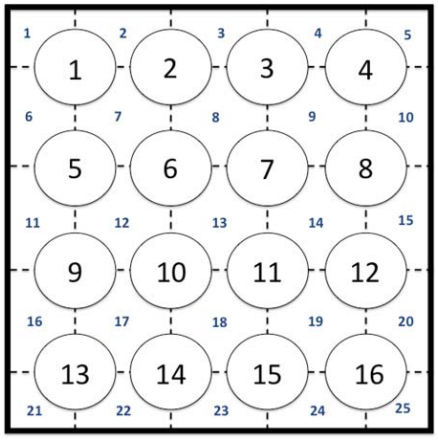

Figure 3: Pin and sub-channel numbering for CTF-DeCART coupled 4x4 sub-assembly models [2]

Figure 3 shows both the pin numbering as well as the coolant sub-channel numbering. A sub-assembly was modeled based on a sub-section of the 17x17 ORNL design used for their AMPFuel code [8] as shown in Figure 4. The DeCART nodalization for the sub-assembly can be found in Figure 4.

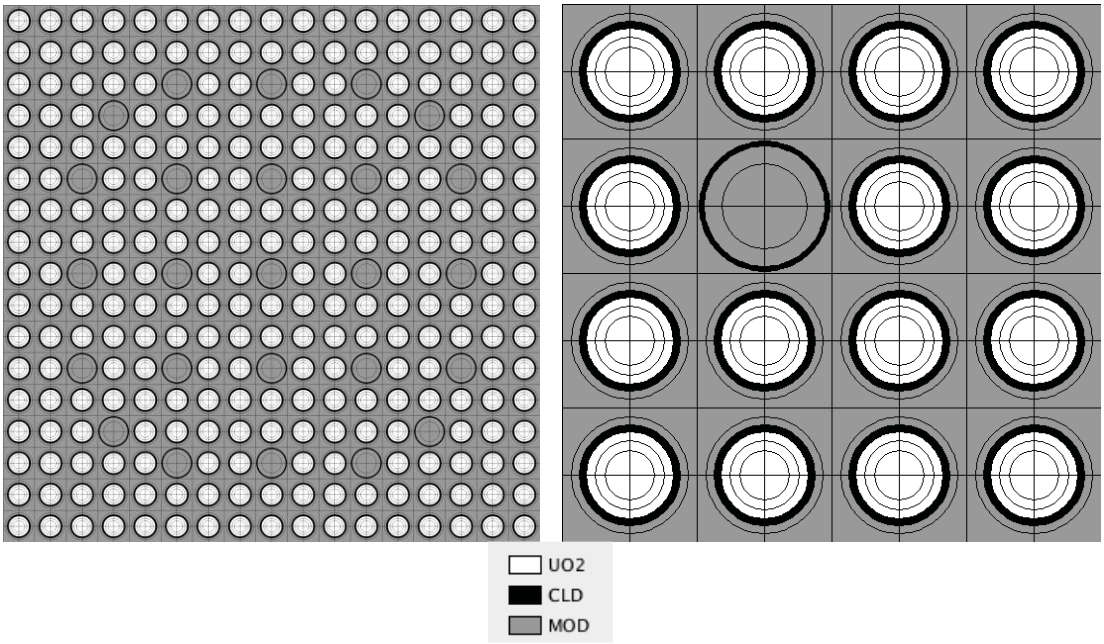

Figure 4: Left: ORNL AMPFuel full 17x17 assembly Right: DeCART nodalization diagram for 4x4 sub-assembly with guide tube [2]

As can be seen in Figure 4, a guide tube for a control rod was placed in position six. To create a large temperature variation, the right side column and bottom row were given a higher enrichment than the other fuel pins. This made the pin in position 11 (starred in Figure 5) the pin of interest. The input parameters used for this sub-assembly coupled calculation are listed in Table 1. A graphical representation of the geometry and enrichment distribution can be found in Figure 5.

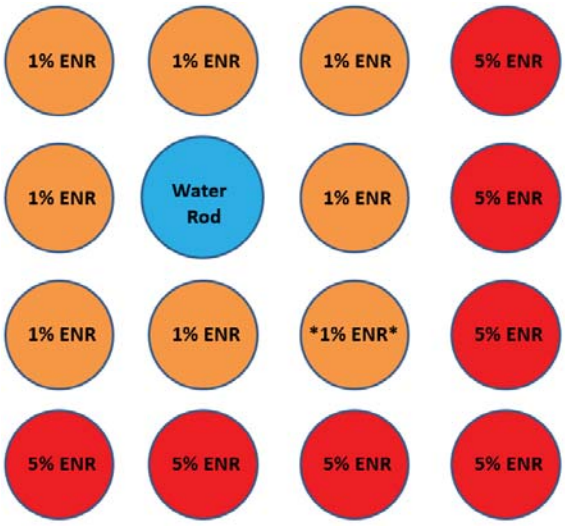

Figure 5: 4x4 Sub-assembly with guide tube layout at 0 MWd/kgU burnup with pin of interest starred

Table 1: CTF-DeCART 4x4 sub-assembly input parameters

Parameter	Value	Units
Reactor	PWR	
Layout	4 x 4	
Fuel	UO_2	
Enrichment		
High	4.95	%
Low	1.00	%
Fuel Density	10.4	g/cm^3
Percent Theoretical Density	95	
Burnable Poison	None	
Cladding	Zircaloy-4	
Cladding Density	6.55	g/cm^3
Coolant	H_2O	
Fill Gas	Helium	
Fill Gas Density	0.0002	g/cm^3
Fuel Pellet radius	4.095E-3	m
Cladding Inner Radius	4.18E-3	m
Cladding Outer Radius	4.75E-3	m
Cladding Thickness	5.70E-4	m
Pin Pitch	1.26E-2	m
Active Fuel Height	3.658	m
Top Reflector Height	0.355	m
Bottom Reflector Height	0.355	m
Array Power	1.00	MW
Average Linear Heat Rate	18.225	kW/m
Core Pressure	15.5	MPa
Mass Flow Rate	4.86	Kg/s
Beginning of Cycle boron loading	1700	ppm
Inlet Temperature	287	°C

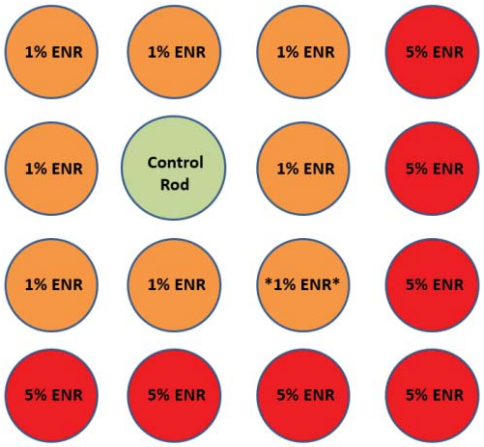

Figure 6: 4x4 Sub-assembly with control rod layout at 0 MWd/kgU burnup with pin of interest starred

The next azimuthally varying temperature case created was a 4x4 sub-assembly in which the guide tube was replaced with a control rod. This was not created to model a physical situation, as commercial PWRs do not operate with rods inserted, but to create an anisotropic system to test the abilities of the code. The input parameters for the control rod case were identical to the 4x4 water rod case, with the only

difference being the guide tube's internal material was boron as opposed to water. Figure 6 shows the x-y planar layout of the sub-assembly.

1.2.2 BISON Model Description

A two-dimensional r-θ BISON model was created to model the pin of interest (pin 11). The model was a 'slice' of the pin at a core height of 1.85 meters. The geometric mesh for the model was created using the TRELIS [9] meshing software. The input deck used the same parameters as the coupled code and the boundary condition applied from the code coupling were time dependent radial power profile of the fuel and a time dependent outer cladding temperatures. The BISON model was then run for the same simulation times that their respective CTF-DeCART models.

1.2.3 Hydrogen Model Description

In a pressurized water reactor under normal conditions, the zirconium cladding can be exposed to varying temperatures with the outer surface constantly in contact with the coolant. This interface at high temperatures facilitates the oxidation of zirconium through the following reaction:

$$Zr + 2H_2O \rightarrow ZrO_2 + 2H_2 \tag{1}$$

Approximately 10-20% of this hydrogen that is produced can be absorbed by the non-oxidized cladding. [10] Although the hydrogen pickup fraction has been shown to vary during corrosion [11], the pickup fraction in this study, for simplicity, is taken to be constant (15%) as the focus is on what happens to the hydrogen once it gets into the cladding. Once in solid solution in the cladding material, the hydrogen can diffuse throughout the cladding driven by gradients in temperature, concentration and stress. This study focuses on the hydrogen fluxes due to concentration and temperature gradients which are described by equations 2 and 3.

$$J_{Fick} = -D\nabla C_{ss} \tag{2}$$

$$J_{Soret} = -\frac{DC_{ss}Q^*}{RT^2}\nabla T \tag{3}$$

Together, these effects can be combined into a single equation for the flux of hydrogen in solid solution of the zirconium:

$$J_D = -\mathrm{D}\nabla C_{ss} - Q^*\frac{DC_{ss}}{RT^2}\nabla \mathrm{T} \tag{4}$$

Where,
J_D is the diffusion flux;
C_{ss} is the concentration of hydrogen in solid solution;
R is the gas constant;
T is the temperature in degree kelvin;
Q* is the heat of transport;
D is the diffusion coefficient of hydrogen in zirconium.

Hydrogen redistribution will be driven by the flux determined from equation 4; clearly in some situations or at any one stage, one term or the other will be dominant. For a more in depth discussion on the governing equations of the hydrogen distribution, see references [12-14]. Once the concentration of hydrogen in solid solution exceeds the hydrogen solubility limit in the α-zirconium matrix, hydrogen may

precipitate as a zirconium hydride. This hydride precipitation is governed by the terminal solid solubility which is determined by the hydrogen concentration and temperature of the cladding (other factors such as irradiation and alloying elements can also affect hydride precipitation, but they are not considered in this model). The precipitated hydrides can dissolve back into solid solution if the concentration of hydrogen later dips below the solubility limit. These limits are known as the Terminal Solid Solubility of precipitation and dissolution (TSSp and TSSd). According to McMinn [15], and without any additional effects, the TSSd and the TSSp in wt. ppm of hydrogen in solid solution can be approximated by the following equations:

$$\begin{cases} TSSd = 106446.7 * exp\left(-\dfrac{4328.67}{T}\right) \\ TSSp = 138746.0 * exp\left(-\dfrac{4145.72}{T}\right) \end{cases} \quad (5)$$

Within this collaboration, a subroutine was created for the BISON code that employed these equations. [12] Given temperature boundary conditions and an initial hydrogen concentration, the code will calculate the spatial distribution of hydrogen and the partition between dissolved hydrogen and precipitated hydrogen (hydrides), as a function of time, as driven by the existing gradients of temperature and concentration.

1.2.4 CTF-DeCART-BISON Hydrogen Distribution Results

1.2.4.1 Guide Tube Sub-Assembly Model Results

The CTF-DeCART coupling modeled a 3D sub-assembly that spanned the entire 3.62 meter active fuel length. However, the BISON model was created as a single two-dimensional (r, θ) model, i.e. an x-y planar cut of a single fuel rod. The CTF-DeCART coupled calculation was executed first. An example of the outer cladding temperature distribution can be seen in Figure 7, where each temperature is the temperature of the corresponding quadrant of the cladding (North East, North West, South East, South West as can be seen in Figure 4). This temperature distribution shown is for the 38th axial COBRA-TF node for the 0 MWd/kgU burnup step (time zero). This vertical node corresponds to the 1.85 m - 1.90 m height in the core (just above the vertical center of the core). For this coupling, DeCART used a different nodalization (18 vertical nodes) meaning this CTF node corresponds to the 10th vertical DeCART node.

578.3 578.2 1% Enr. 578.2 578.5	578.0 577.7 1% Enr. 578.3 577.9	576.9 583.9 1% Enr. 577.0 583.8	607.4 614.7 4.95% Enr. 607.3 614.5
578.0 578.2 1% Enr. 577.6 577.8	566.5 566.1 Guide Tube 566.1 565.7	576.8 583.6 1% Enr. 576.5 583.1	606.7 613.8 4.95% Enr. 606.2 613.2
576.7 576.8 1% Enr. 583.9 583.7	576.7 576.4 1% Enr. 583.6 583.2	575.7 582.6 1% Enr. 582.5 585.4	604.6 611.6 4.95% Enr. 607.5 610.6
607.1 607.0 4.95% Enr. 614.4 614.3	606.4 605.9 4.95% Enr. 613.7 613.0	604.4 607.3 4.95% Enr. 611.5 610.5	605.6 608.8 4.95% Enr. 608.8 608.2

Figure 7: Azimuthal outer cladding temperatures (deg. K) for CTF axial node 38 (near the vertical center of the core) at 0 MWd/kgU with the temperature distribution of interest boxed in white

The rod selected to run in the BISON simulation was rod 11 (boxed in white on Figure 7) as it showed the largest azimuthal variation in temperature.

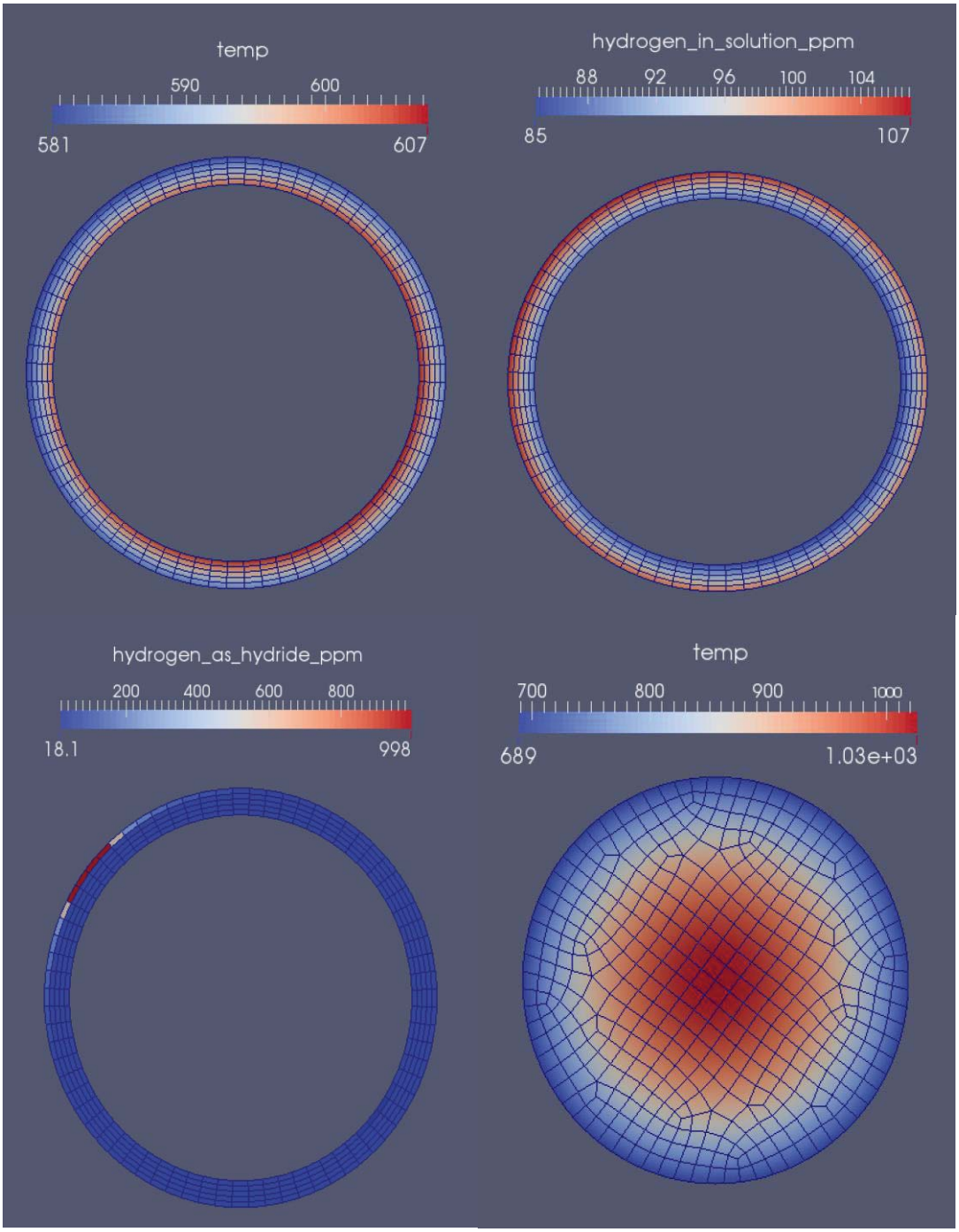

Figure 8: Rod 11 1.85 m height BISON output at 3.43E7 seconds *Top Left*: **Cladding temperature (K)** *Top Right:* **Cladding hydrogen distribution** *Bottom left:* **Cladding hydride distribution** *Bottom Right:* **Fuel temperature (K)**

Figure 8 shows the end of simulation temperature distribution within the cladding and fuel with respect to distance across the largest temperature gradient. As seen in equation 6,

$$TSSp_{water\_rod} = 138745.0 \exp\left(-\frac{4145.72}{581}\right) = 110\ wt.ppm \quad (6)$$

there should not be any hydrides within the cladding. There is, however, a small amount of hydrogen in the form of precipitated hydride in the North West quadrant. This concentration was likely caused due to the temperature at that location having decreased far enough that the C_{ss} went below the TSSp so that the hydride precipitation could occur. Once precipitation occurred, the concentration in that small volume increased up to the maximum allowed concentration (1000 wt. ppm). According to the model, this would be the mechanism of formation of a hydride rim under a temperature gradient. Given more time, a hydride rim would likely be seen as more hydrogen will be picked up by the cladding. However, the actual rim microstructure is more complex that what is shown. Note that after precipitating the concentration of hydrogen in solid solution decreases and falls below the TSSp. When calculating the TSSd for this location:

$$TSSd_{water\_rod} = 106446.7 \exp\left(-\frac{4328.67}{581}\right) = 62\ wt.ppm \quad (7)$$

it becomes apparent that the criteria for dissolution is also met, but not in the hysteresis region. This confirms why there would be a small amount in this cold region.

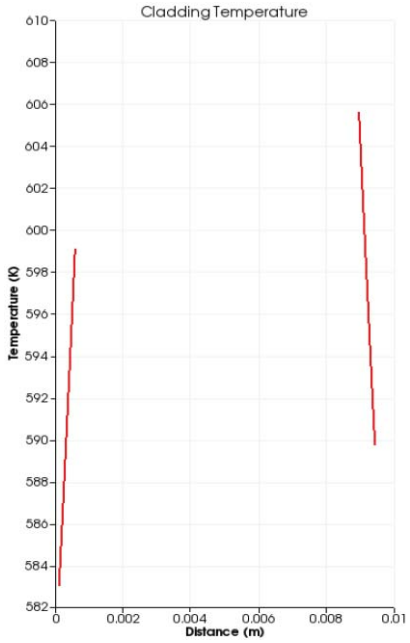

Figure 9: Rod 11 axial height 1.85-1.90 m end of simulation BISON radial cladding temperature distribution

1.2.4.2 Control Rod Sub-Assembly Model Results

This same calculation was performed for a shorter simulated operation time in BISON, 1.1 x 10^7 seconds (a little over four months) as compared to 3.4 x 10^7 (about a year) in the previous case. In this simulation the guide tube was replaced with a control rod. The results at the end of 1.1 x 10^7 seconds are shown in Figure 10. It can be seen that there was no concentration of hydrides. This is due to the conditions in the core not allowing enough hydrogen absorption in the cladding to exceed the TSSp which is the minimum requirement for precipitation of hydrogen anywhere in the cladding. For the lowest temperature of the cladding, the TSSp has a value of

$$TSSp_{control\_rod} = 138745.0 \exp\left(-\frac{4145.72}{583}\right) = 113\ wt.ppm \quad (8)$$

The reason why the concentration of hydrogen in solid solution is lower compared to that seen in the water rod case in the previous section is that the simulation time was shorter, which did not allow for enough time for hydrogen to accumulate in the cladding. Figure 11 shows the temperature distribution within the cladding with respect to distance across the largest temperature gradient.

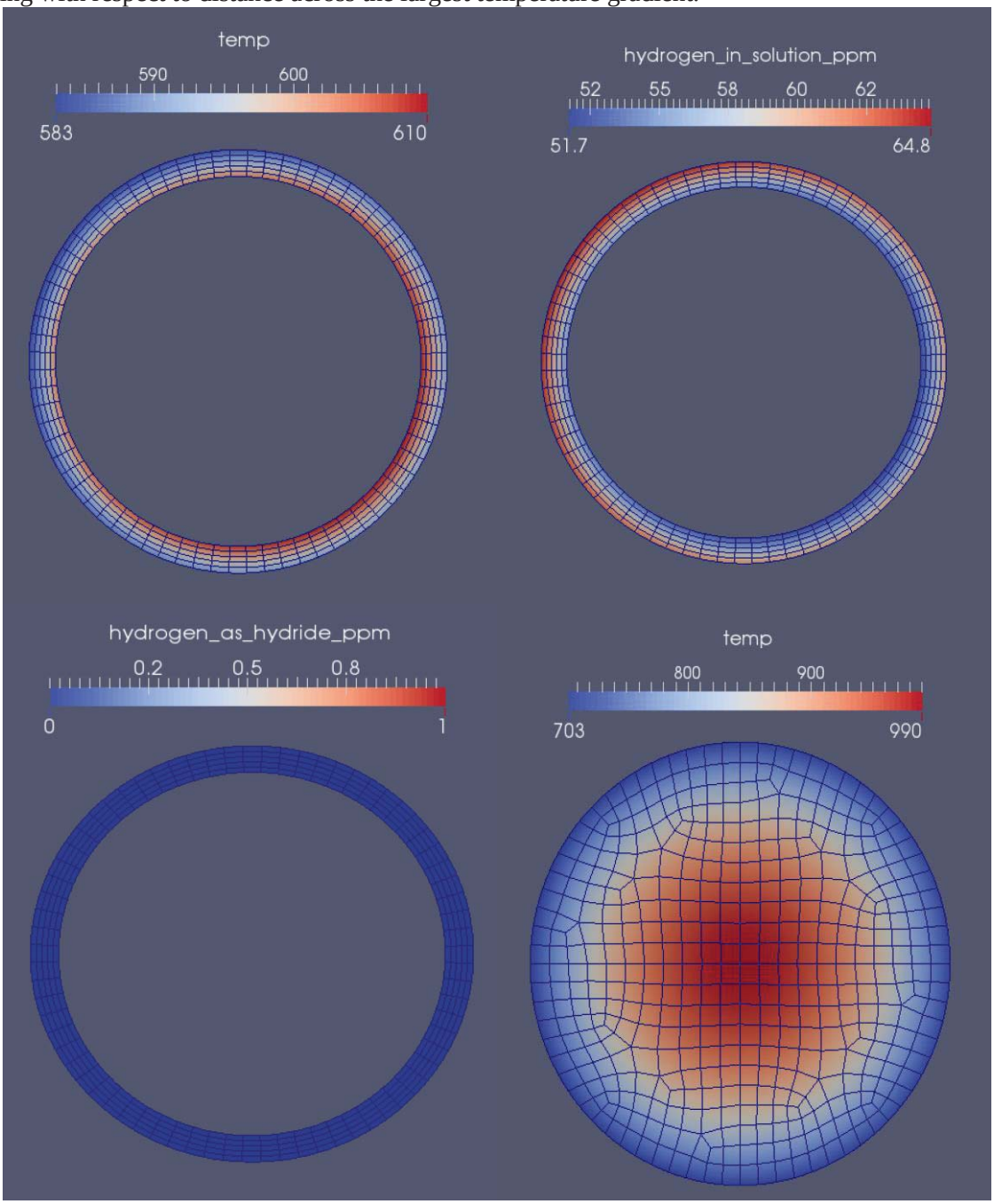

Figure 10: Rod 11 1.85 m height BISON output with control rod in assembly at 11E6 seconds *Top Left:* **Cladding temperature distribution** *Top Right:* **Cladding hydrogen distribution** *Bottom left:* **Cladding hydride distribution** *Bottom Right:* **Fuel temperature**

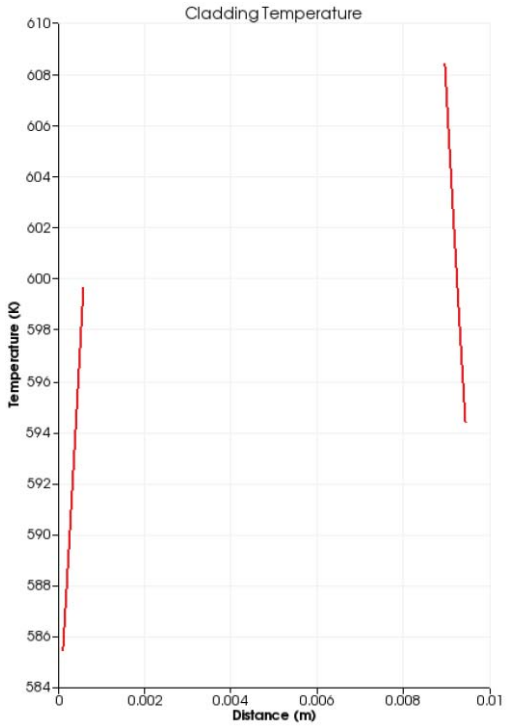

Figure 11: Rod 11 axial height 1.85-1.90 m end of simulation BISON radial cladding temperature distribution for the control rod case

1.3 CTF-DeCART to CTF-MPACT Comparisons

Before continuing the project with the alternate multi-physics coupling scheme (MPACT-CTF), several cases were used to compare the CTF-DeCART coupling with the CTF-MPACT coupling. The first model was a simple 4x4 sub-assembly consisting of only fuel pins. Both models used the input parameters found in Table 1, with several changes. The enrichment was 3.45 weight percent for the entire sub-assembly, and the beginning of cycle boron loading was 1000 ppm. The first parameter compared between couplings was the axial power profile of a single pin. The pin in position 7 was chosen and the normalized axial power profile versus axial height is shown in Figure 12.

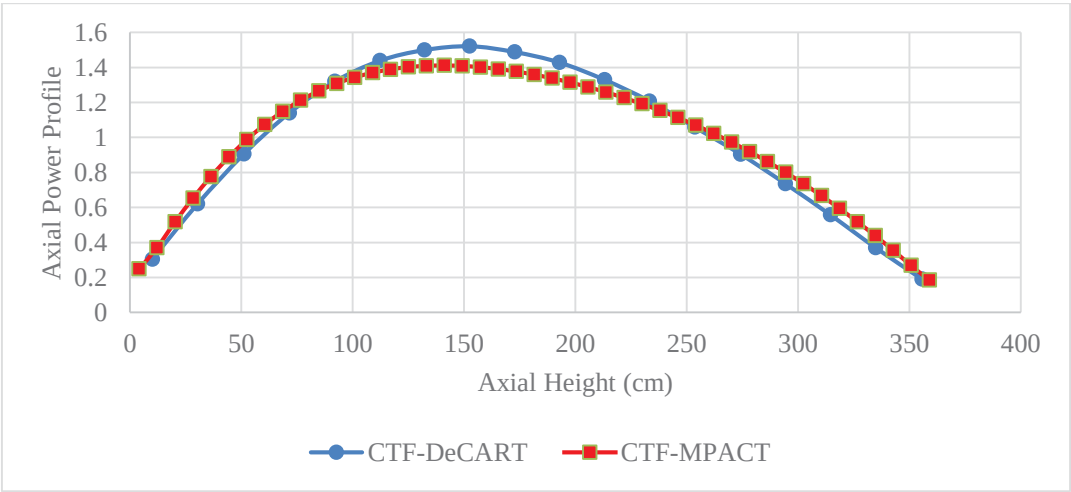

Figure 12: Axial power profile vs. axial height for pin 7 for 4x4 fuel pin array at 0 MWD/MTU

From Figure 12, the maximum absolute difference in the axial normalized power profile between the two coupled codes was 0.1156 or 8.2% difference. The average absolute difference in the axial normalized power profile was 0.0601. Several factors can be attributed to the differences seen between the coupled codes. First, while both codes use a 47 group energy group cross sections library, as discussed in section 1.1, the cross section libraries are different. Additionally, CTF-MPACT is an internal coupling whereas CTF-DeCART is externally coupled and CTF-MPACT passes more information between the codes. An additional difference to be noted, the CTF-DeCART code allows for differing axial mesh sized between the DeCART and CTF. An averaging scheme was used to pass values back and forth for the differing mesh sizes.

Next, the same 4x4 sub-assembly model was used, but pin 6 was replaced with a guide tube and the power was decreased to 1.01325MW. The normalized radial power distributions for each code coupling at 0 MWD/MTU burnup are found in Table 2. The maximum absolute difference in this instance was 0.0103 and the average absolute difference was 0.0038.

Table 2: *Left:* **CTF-MPACT (top values) and CTF-DeCART (bottom values) axially integrated 2D power for 4x4 array with guide tube. 0 MWD/MTU.** *Right:* **Difference between CTF-MPACT and CTF-DeCART**

1.0337 **PIN 1** 1.0243	1.0454 **PIN 2** 1.0447	1.0061 **PIN 3** 1.0060	0.9875 **PIN 4** 0.9804
1.0454 **PIN 5** 1.0449	0.0000 **GUIDE TUBE**	1.0211 **PIN 7** 1.0248	0.9763 **PIN 8** 0.9812
1.0061 **PIN 9** 1.0064	1.0211 **PIN 10** 1.0250	0.9855 **PIN 11** 0.9926	0.9701 **PIN 12** 0.9714
0.9875 **PIN 13** 0.9810	0.9763 **PIN 14** 0.9816	0.9701 **PIN 15** 0.9716	0.9680 **PIN 16** 0.9640

0.0103	0.0007	0.0001	0.0071
0.0005	0.0000	-0.0037	-0.0049
-0.0003	-0.0039	-0.0071	-0.0013
0.0065	-0.0053	-0.0015	0.0040

2 CONCLUSIONS

The reactor environment, in which nuclear fuel operates, requires improved multi-dimensional fuel and cladding simulation and analysis to accurately describe fuel behavior. The behavior of hydrogen in the fuel is an important factor in fuel behavior, and the development of high fidelity coupled codes allows increased accuracy in temperature distributions that can be used to model the behavior of hydrogen. The hydrogen modeled in BISON has been demonstrated for r-θ direction temperature gradients. This model has been demonstrated in the r-z direction as well (see references [2] and [3]). The model shows expected results and behavior that accurately models the physics in the R-Theta direction. The hydrogen model is under continuing development at INL. The accuracy of the Penn State DeCART-CTF coupling has been shown with a comparison to the MPACT-CTF coupling. Differences are expected to have arisen to differing cross section libraries and modeling constraints. Comparison to experimental data will be performed once detailed hydride precipitation data, including detailed and accurate position and power history data, becomes available.

3 ACKNOWLEDGMENTS

This research was funded by DOE NEUP project 11-2987 and project 13-5180 of the US Department of Energy with extensive contributions by Jason Hales, Ian Davis and Olivier Courty. We would like to thank Matthew Lindenberg at Penn State for his help in configuring BISON.

4 REFERENCES

1. J. D. Hales, S. R. Novascone, G. Pastore, D. M. Perez, B. W. Spencer, R. L. Williamson. BISON Theory Manual: p. 5. Idaho National Laboratory. June 2014.
2. I. Davis. *High-Fidelity Multi-Physics Coupling For Prediction of Anisotropic Power and Temperature Distribution in Fuel Rod: Impact on Hydride Distribution.* 2013. M.Sc. thesis in Nuclear Engineering. The Pennsylvania State University
3. O. Courty. Hydrogen Distribution In Zircaloy Under A Temperature Gradient: Modeling, Simulation And Experiment. 2013. M.Sc. thesis in Nuclear Engineering. The Pennsylvania State University.
4. B. Kochunas, M. Hursin, T. Downar, "DeCART-v2.05 Theory Manual," University of Michigan. 2009.
5. "CTF- A Thermal Hydraulics Sub-channel Code for LWRs Transient Analysis User's Manual," The Pennsylvania State University Department of Mechanical and Nuclear Engineering. Fall 2014.
6. M. Avramova, R. Salko. "CTF Theory Manual" The Pennsylvania State University Department of Mechanical and Nuclear Engineering. April 25, 2014.
7. B. Kochunas, D. Jabaay, B. Collins, T. Downar, "Demonstration of Neutronics Coupled to Thermal Hydraulics for a Full-Core Problem using COBRA-TF/MPACT," CASL Document CASL-U-2014-0051-000, April 1, 2014.
8. S. Hamilton, K. Clarno, B. Philip, M. Berrill, R. Sampath, S. Allu., *Integrated Radiation Transport and Nuclear Fuel Performance for Assembly-Level Simulations*, in *PHYSOR 2012* Knoxville, TN.
9. "Trelis 15 Mesh Generation Software," http://www.csimsoft.com/trelis.jsp (2014)
10. IAEA, "Waterside Corrosion of Zirconium Alloys in Nuclear Power Plants," International Atomic Energy Agency, Vienna IAEA-TECDOC-996, 1998.
11. A. Couet, A. T. Motta, and R. J. Comstock, "Hydrogen Pickup Measurements in Zirconium Alloys: Relation to Oxidation Kinetics," Journal of Nuclear Materials, 451, (2014) 1-13.
12. O. Courty, A. T. Motta, and J. D. Hales, "Modeling and simulation of hydrogen behavior in Zircaloy-4 fuel cladding," Journal of Nuclear Materials, 452, (2014) 311-320.
13. C. Dances, C. Piotrowski, M. Mankosa, A. Motta, M. Avramova, and K. Ivanov, "Anisotropic Azimuthal Power and Temperature Distribution: Impact on Hydride Distribution", Transactions of the 2014 ANS Winter Meeting and Nuclear Technology Expo, November 9-13, 2014, Anaheim, CA.
14. I. J. Davis, O. F. Courty, M. N. Avramova, A. T. Motta, and K. N. Ivanov, "High-Fidelity Multi-Physics Coupling for Prediction of Anisotropic Power and Temperature Distributions in Fuel Rod:

Impact on Hydride Distribution.” The 15th International Topical Meeting on Nuclear Reactor Thermal-Hydraulics, NURETH-15, 491, May 2013, Pisa, Italy.

15. A. McMinn, E. C. Darby, and J. S. Schofield, "The terminal solid solubility of hydrogen in zirconium alloys," 12th ASTM Int. Symp. on Zr in the Nuclear Industry, ASTM STP-1354, Toronto, CA, 2000, 173-195.